



A revised dependence of the edge tone frequency for the first hydrodynamic mode

A. Bamberger^a and D. Ronneberger^b

^aPhys. Institute of Albert-Ludwig-Universität, Hermann-Herder-Str.3, 79104 Freiburg, Germany

^bThird Physics Institute Georg-August-Universität, Friedrich-Hund-Platz 1, 37077 Göttingen, Germany
bamberger@physik.uni-freiburg.de

The first hydrodynamic mode of the edge tone according to various publications over the years seemed to have a different behavior of the frequency f as a function of the stand-off distance L being $f \propto 1/L$ relationship, in contrast to the higher hydrodynamic modes which tend to have relationship as $1/L^{3/2}$. However a correction is appropriate due to the center of the feedback dipole field at $x = L + \Delta L$. A new analysis of the precise data opens the possibility to assess a power being different from either $n=1$ or $n=3/2$. A global fit to the data with various jet thicknesses determines the ΔL and the power n according to $f \propto 1/(L + \Delta L)^n$. The result shows that the ΔL is in the order of the flue height and n has a value of ≈ 1.3 . Numerical simulations support the insertion ΔL in the analysis. This result is interesting in view of the theoretical deduction of the edge tone by Crighton which should be modified by an appropriate evaluation of the dispersion relation and thus changing for Crightons relation the power from $3/2$ to 1.26 , in agreement with the experimental findings.

1 Introduction

The edge tone is investigated in numerous papers with the medium air as well as water. Several papers are dealing with this phenomenon from the point of view of experiment, theoretical treatment and simulation. It is also relevant for the instantaneous speaking of a organ pipe by adjusting the cut-up so that the edge tone matches some partial of the resulting sound. A better understanding based on precise measurements was achieved as the additional extension of the stand-off length L was introduced with the notion that the dipole source is not right on the tip, but some effective distance ΔL beyond the edge [1, 8, 6, 5].

The findings of simple dependence for the first hydrodynamic mode generally as $f \propto 1/L$ for different flue height and corresponding simulation in the paper of one of the authors [3]. In detail for $d = 0.5\text{mm}$ a power of $n = 1.10 \pm 0.04$ for the $f \propto 1/L^n$ is also quoted there. Already at that time the experimental data being referred to by several authors show that the power n does depend on the hydrodynamic mode in such a way that the first mode had a power $n < 3/2$ [2], and even more striking six years later citing experimental data in comparison to theoretical knowledge [4]. The present contribution deals with a simultaneous determination of

$$L' = L + \Delta L \text{ and the power } n.$$

The result produces, to the knowledge of the author for the first time, an insight to the validity of Crightons theoretical deduction of the edge tone relationship which assumes a low frequency approximation. The extension towards Strouhal numbers in the order of 1 results in an essential modification being appropriate for this experiment. The experimental edge tone data of the first hydrodynamic mode is commonly terminated in range of L by the jump into the higher hydrodynamic mode, so precision data are required.

2 The experimental method and data taking

The geometry was designed to be close to a flute-like flue labium configuration because of interest in flute-like instruments. The channel height of $d = 1.0\text{mm}$ can be modified to 0.5mm , see Fig. 1. The span-wise extension is 10mm . In order to achieve a parabolic velocity profile the length was chosen safely to be 150mm . The edge with an angle of 23° is mounted on a movable table allowing a precision setting in the $50\mu\text{m}$ range. The pressure signal on the upper surface of the wedge is measured by a sensor coupled to the flow close to tip of the edge (Kulite 9332M).

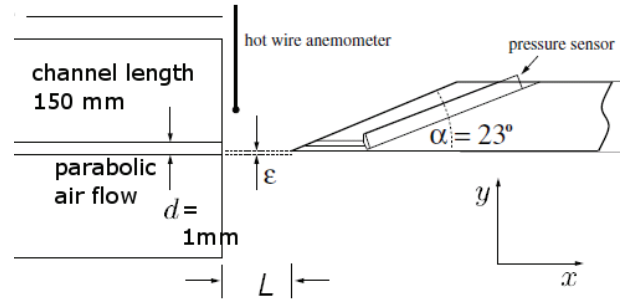


Figure 1: Experimental setup for the edge tone measurement.

The setup was positioned at $\sim 20\text{cm}$ above the mounting table. The micro-meter adjustment in height was in general $\epsilon \approx 1/4$ of the channel height by maximizing the pressure signal.

The velocity measurement was achieved with a hot-wire anemometer (Dantec C35). During the data taking the anemometer was retracted. The calibration was done with a Pitot tube. The accuracy of the calibration is estimated as $\pm 0.5\text{m/s}$. Because of its sensitivity to environmental temperature changes constant temperature was required. For the frequency determination of the fundamental mode f a spectral analyzer was employed (Tektronix 2642A) with a precision of $< 1\%$.

The velocity profile of the jet was checked to be parabolic without wings 1mm downstream from the flue exit, also for a smaller channel length $\sim 100\text{mm}$ of the flue. A check with the Schlieren method revealed that the jet is quasi laminar.

In Fig. 2 the measurements are presented on top for the data with $d = 0.5\text{mm}$ and below for the data with $d = 1.0\text{mm}$. The fits are obtained by $f \propto 1/L$. Especially for $d = 0.5\text{mm}$ the data exhibit a slightly steeper slope than -1 which could be attributed to a power $n > 1$. The velocities listed are the maximum of the profile U_0 and used further on. Both distributions show in the log-log plot a negative curvature as a function of L , especially for the $d = 0.5\text{mm}$ case. This fact indicates that the dependence on L should be modified by a possible displacement of the dipole source from the edge ΔL [1, 8, 6, 5].

3 Fits for ΔL and n all data individually for each U_0

For the fits onto the data the function $f/U_0 \propto 1/(L + \Delta L)^n$ with the following parameters ΔL which is a correction of

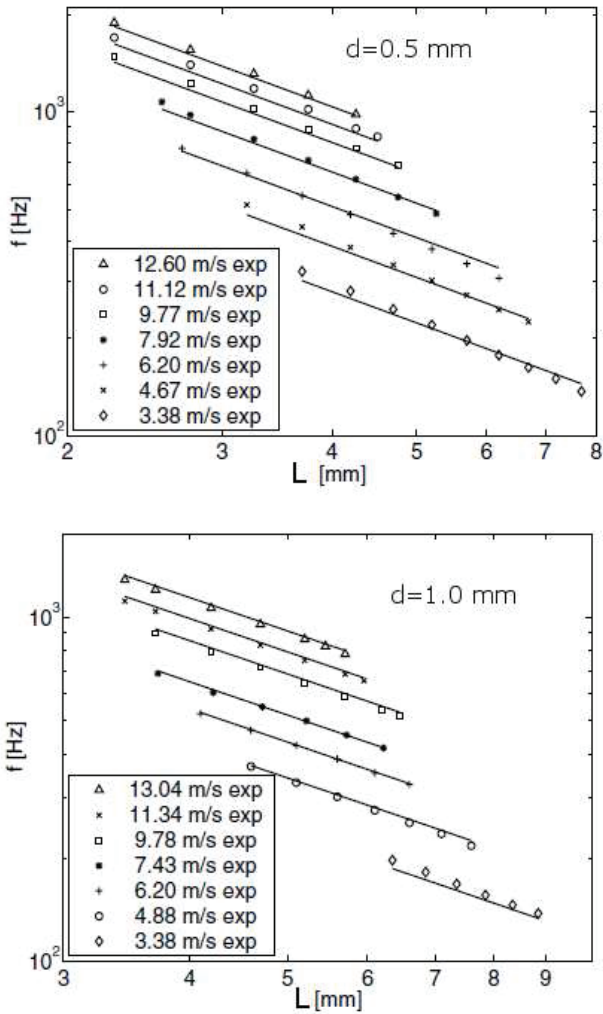


Figure 2: The data set is shown as published [3]. The frequency f is displayed as a function of the stand-off distance L for two flue heights $d=0.5$ (upper part) and $d=1.0$ mm (lower part). The fits provide the guide of eye with the function $f \propto 1/L$. A closer look especially at $d=0.5$ mm reveals that the data overshoot at small L and undershoot at large stand-off distance.

the stand-off distance and n the power. For each data set f/U_0 at a given U_0 a multiplicative constant is associated with in order to yield a reasonable χ^2 . Moreover, considering the uncertainty of the velocity determination being dominant compared with other uncertainties a global 5% error is assigned. An evaluation of the constants in view of the different flue height of $d=0.5$ mm and $d=1.0$ is interesting, however not followed up in this presentation.

Having performed preliminary fits with fixed values for either ΔL or n at expected values, as $0.5 < \Delta L < 1.0$ mm or $1 < n < 3/2$, it was found that a common fit for all parameters is possible. In fact, the ΔL shows up at small L whereas the power n dominate at large L which helps to achieve a minimum in χ^2 . The results of the relevant parameters along with their errors are documented in Fig. 3 and Fig. 4 for $d=0.5$ mm and $d=1.0$ mm, respectively.

Finally the average over velocities from error weighted results of ΔL and n are listed in Table 1.

The stability of the fits is sufficient to reach a χ^2 minimum. It should be noted that there is some positive

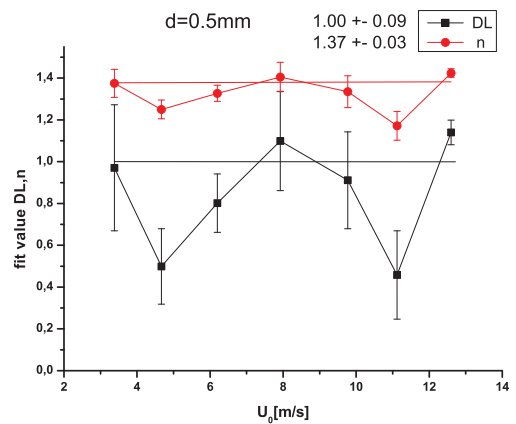


Figure 3: The parameters ΔL and n as a function of the velocity along with its errors are presented for $d=0.5$ mm. The weighted mean and its errors are quoted in the header.

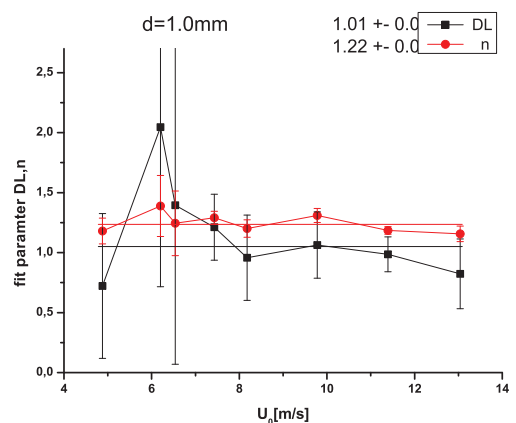


Figure 4: The equivalent of Fig. 3 showing the parameters ΔL and n for $d=1.0$ mm. The large error bars at $U_0=6.5$ m/s are understood by the data structure.

flue height mm	ΔL mm	error mm	n	error
$d=0.5$	1.00	± 0.09	1.37	± 0.03
$d=1$	1.01	± 0.05	1.22	± 0.02

Table 1: The fit parameters of the overall constant for a given velocity the displacement of the effective position of dipole source beyond the tip of the edge ΔL and as a main result the power n .

correlation between ΔL and n , which is expected given the finite range of the edge tone signal in L as explained above. The correlation of ΔL and n is positive with a ratio of about 5:1, what makes the determination of n trustworthy. The results were cross checked with the ROOT-fitting routine.

4 Plot of data and numerical simulation in terms Sr_L

4.1 Experimental results

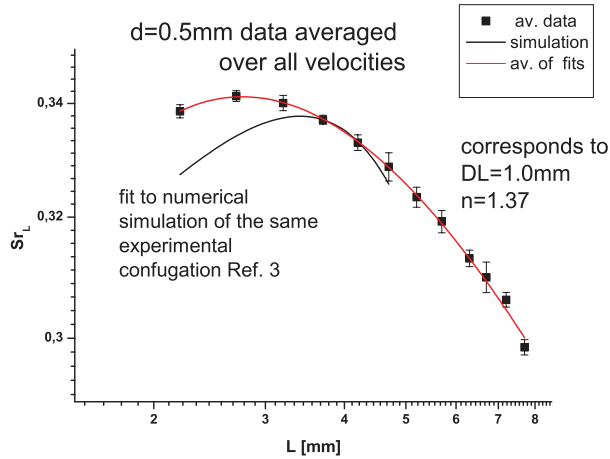


Figure 5: The data set Sr_L is displayed for $d=0.5$ mm. The negative curvature at $2 < L < 4$ is indicating that an added ΔL to the stand-off distance results in a continuous change of the slope. The asymptotic power of $n - 1 = 0.37$ being a straight line in this plot is reached only far beyond $L=8$ mm.

The solid line which represents the averaged Strouhal numbers of the numeric simulation for $d=0.5$ mm and which is based on a 2^{nd} -order polynomial fit is adjusted in scale to the experimental data.

In order to demonstrate the dependence of f on the stand-off distance L for different velocities U_0 the normalized frequency called Strouhal number $Sr_L = fL/U_0$ is shown in Fig. 5 for $d=0.5$ mm and in Fig. 6 for $d=1.0$ mm. In this log-log plot the velocity averaged data show a maximum as a function of $\log(L)$ signaling a deviation from a power law $\log(f) = n\log(L) + \text{const}$ at low L since in a log-log plot Sr_L versus L would appear as a straight line $\log(Sr_L) = (1 - n)\log(L) + \text{const}$. The modification of the argument with the constant ΔL results in

$$\log(Sr_L) = \log \frac{L}{(L + \Delta L)^n} + \text{const} \quad (1)$$

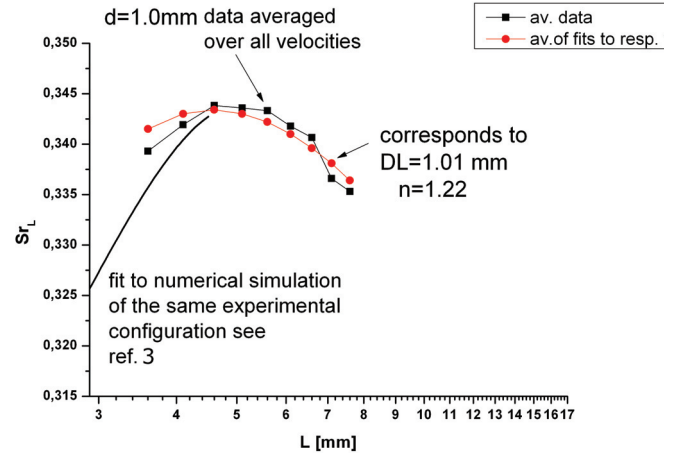


Figure 6: The data set Sr_L is displayed for $d=1.0$ mm. There is a similar change of the slope as a function of L as for $d=0.5$ mm. Note that the limit of the L -scale are adjusted so that scaling of the abscissa as L/d is mimicked. The solid line indicates the averaged Strouhal numbers of the numeric simulation which has the correct positive slope. The Sr_L^{sim} is scaled up by 30% for this comparison.

Compared to the power law the effect is a diminishing slope going from large to small L . It creates a maximum at a stand-off distance $\Delta L/(n - 1)$, as seen in Fig. 5 at $L=2.7$ mm and in Fig. 6 at $L=4.6$ mm.

The case of $d=0.5$ mm indicates that a perfect fit to the data also at small L is achieved by inserting the displacement ΔL which is interpreted as an effective dipole source position beyond the edge. This notion has been mentioned in several publications [1, 8, 6, 5].

A similar observation is shown for $d=1.0$ mm in Fig. 6. In contrast to the data for $d=0.5$ mm a continuation far beyond the maximum with increasing L is excluded because the jump to the second hydrodynamic mode occurs at $L=8$ mm.

Note that the abscissa in Fig. 6 is expanded by a factor of 2. So the abscissa extends to identical ranges of L/d in both the Figures 5 and 6 according to a proper scaling of the stand-off distance. Indeed the maximum of Sr_L appears at comparable L/d for $d=0.5$ mm and $d=1.0$ mm.

4.2 Numeric simulations

The publication includes numerical simulations as a major part [3]. The geometrical setup of the apparatus was exactly implemented, except that the simulation was done in a 2-dimensional model. The main ingredients are refined grid structure at edges and the exact divergence treatment according to the *Babuska – Brezzi* condition at each cell.

Here 2^{nd} -order polynomial fits to both the sets of the resulting Sr_L are shown as solid lines in the Figures 5 and 6. In fact the simulation reproduces the characteristic shape near the maximum in the log-log plot for $d=0.5$ mm. For the $d=1.0$ mm case the simulation was not pursued far enough to reach the maximum in this plot, nonetheless the slope appears to be in fair agreement with the experimental data. For comparison reasons the simulated Sr_L were scaled up by about 30%.

Finally it should be stressed that the asymptotic power law $1/L^{n-1}$ is approached only at very large L which is

not observable because of being the regime of higher hydrodynamic modes. Fortunately, the smaller jet height of $d=0.5\text{mm}$ serves as an indication of the separation of the ΔL dominated regime from the onset of the asymptotic regime.

5 Modification of power dependence and change in final relationship according to Crighton

5.1 Crightons result 1992

Crighton [2] introduces several simplifications mainly concerning the geometry of the flow as well as the interaction between the flue exit and the edge in order to enable an exact treatment of the jet-edge problem. He mentions a fair agreement between his prediction $Sr_{d/2} \propto 1/L^{3/2}$ and experimental data available at that time, except for the proportionality factor which is much too high in the theoretical result. Crighton finds out that the main reason for this discrepancy is the asymptotic phase velocity of the jet instability $c_{ph} = 2U_0Sr_{d/2}^{1/3}$ which is valid only at extremely low frequencies but is nevertheless adopted in the theory. So he ends up with

$$Sr'_{d/2} = \frac{2\pi fd}{2U_0} = (d/2L)^{3/2}(4\pi(N - 3/8))^{3/2} \quad (2)$$

$$Sr'_L = \frac{2\pi fL}{2U_0} = (d/2L)^{1/2}(1.8\pi(N - 3/8))^{3/2} \quad (3)$$

5.2 Modification of Crightons result

With a numerical evaluation of the dispersion relation $c_{ph} \approx 0.9U_0Sr_{d/2}^{0.21}$ is obtained in the range of the experimentally observed Strouhalnumbers $0.05 < Sr_{d/2} < 1$. Replacing the asymptotic phase velocity by this more realistic value yields

$$Sr'_{d/2} = \frac{2\pi fd}{2U_0} = (d/2L)^{1.26}(1.8\pi(N - 3/8))^{1.26} \quad (4)$$

$$Sr'_L = \frac{2\pi fL}{2U_0} = (d/2L)^{0.26}(1.8\pi(N - 3/8))^{1.26} \quad (5)$$

instead relation (2,3). The relations (4,5) are the appropriate ones to be compared with this experiment within the range of Strouhal numbers according to our definition in this contribution $Sr_L = fL/U_0 < 0.4$. Based on the results presented in Fig. 5 and Fig. 6 also L is to be replaced by $L' = L + \Delta L$.

6 Conclusion

In this investigation extended fits are done onto the data with the following modifications.

1. The displacement of the effective dipole source position is added to the stand-off distance L with the result $\Delta L_{d=0.5} = 1.00\text{mm}$ and also $\Delta L_{d=1.0} = 1.01\text{mm}$. The value for $d=0.5$ changes with other possible weighting resulting in $\Delta L_{d=0.5} = 0.8\text{mm}$. From estimations [8] the ratio $\Delta L_{d=0.5}/\Delta L_{d=1.0} \approx 1/2$ is expected.

2. The numeric simulation supports the findings of this modification by reproducing the bump structure for Sr_L especially for the $d=0.5\text{mm}$ data.
3. The main result of the fits for $d=0.5\text{mm}$ and $d=1.0\text{mm}$ is $n_{d=0.5} = 1.37 \pm 0.03$ and $n_{d=1.0} = 1.22 \pm 0.03$, the above value based on the dispersion relation of $n_{theor} = 1.26$ within 9%.

This evaluation of the edge tone of the fundamental hydrodynamic mode demonstrates for the first time, to the knowledge of the authors, a dependence of the frequency of $f \propto 1/(L + \Delta L)^n$ close to the theoretical value of $n=1.26$ which is a justified modification of the relation published by Crighton in 1992[2]. It should be noted that this power is expected to hold for many similar experiments dealing with the first stage, including those using water as a medium for the edge tone excitation.

References

- [1] Powell, A., "On the edge tone" JASA 33, 395(1961)
- [2] Crighton D. G., "The jet edge-tone feedback cycle; linear theory for operating stages" Journal of Fluid Mechanics 234, 361(1992)
- [3] Bamberger, A. et al., "Experimental and numerical investigations of edge tones" Journal of applied Mathematics and Mechanics 84, 632 (2004)
- [4] Howe, M. S., "Acoustics of fluid-structure Interaction", Cambridge University Press, 1998, chapter 6.3.1, Fig. 6.3.4 on page 476
- [5] Kwon, Young-Pil, "'Feedback mechanism of low-speed edgetones'" JASA 104(4) 2084 (1998)
- [6] Ausserlechner et al., "Experimental jet velocity and edge tone investigations on a foot model of an organ pipe" JASA 126, 878 (2009)
- [8] Verge, J.-P. et al., "Sound production in recorder like instruments II" JASA 101, 2925 (1997)